

RESEARCH ARTICLE

Hemocyanin with phenoloxidase activity in the chitin matrix of the crayfish gastrolith

Lilah Glazer^{1,2}, Moshe Tom³, Simy Weil¹, Ziv Roth^{1,4}, Isam Khalaila⁴, Binyamin Mittelman^{1,2} and Amir Sagi^{1,2,*}

¹Department of Life Sciences, Ben-Gurion University of the Negev, Beer Sheva 8410501, Israel, ²National Institute for Biotechnology in the Negev, Ben-Gurion University of the Negev, Beer Sheva 8410501, Israel, ³Israel Oceanographic and Limnological Research, Haifa 8511911, Israel and ⁴Avram and Stella Goldstein-Goren Department of Biotechnology Engineering, Ben-Gurion University of the Negev, Beer Sheva 8410501, Israel

*Author for correspondence (sagia@bgu.ac.il)

SUMMARY

Gastroliths are transient extracellular calcium deposits formed by the crayfish *Cherax quadricarinatus* von Martens on both sides of the stomach wall during pre-molt. Gastroliths are made of a rigid chitinous organic matrix, constructed as sclerotized chitin–protein microfibrils within which calcium carbonate is deposited. Although gastroliths share many characteristics with the exoskeleton, they are simpler in structure and relatively homogeneous in composition, making them an excellent cuticle-like model for the study of cuticular proteins. In searching for molt-related proteins involved in gastrolith formation, two integrated approaches were employed, namely the isolation and mass spectrometric analysis of proteins from the gastrolith matrix, and 454-sequencing of mRNAs from both the gastrolith-forming and sub-cuticular epithelia. SDS-PAGE separation of gastrolith proteins revealed a set of bands at apparent molecular masses of 75–85 kDa; mass spectrometry data matched peptide sequences from the deduced amino acid sequences of seven hemocyanin transcripts. This assignment was then examined by immunoblot analysis using anti-hemocyanin antibodies, also used to determine the spatial distribution of the proteins *in situ*. Apart from contributing to oxygen transport, crustacean hemocyanins were previously suggested to be involved in several aspects of the molt cycle, including hardening of the new post-molt exoskeleton *via* phenoloxidation. The phenoloxidase activity of gastrolith hemocyanins was demonstrated. It was also noted that hemocyanin transcript expression during pre-molt was specific to the hepatopancreas. Our results thus reflect a set of functionally versatile proteins, expressed in a remote metabolic tissue and dispersed *via* the hemolymph to perform different roles in various organs and structures.

Key words: Crustacea, Decapoda, extracellular matrix, cuticle, sclerotization.

Received 2 October 2012; Accepted 30 January 2013

INTRODUCTION

Arthropods, comprising the largest group of animal species, possess rigid exoskeletons composed of an organic matrix consisting of chitin–protein microfibrils (Blackwell and Weih, 1980; Lowenstam and Weiner, 1989). These microfibrils form a network of chitin–protein layers that are helicoidally stacked into a twisted plywood pattern (Bouligand, 1972; Raabe et al., 2005). The rigidity of the exoskeleton is achieved through sclerotization, namely the enzymatic oxidation of phenols or catechols, which then crosslink with and harden cuticular proteins and chitin (Kuballa and Elizur, 2008). In most crustacean species, exoskeletons are further hardened by the deposition of minerals, mainly calcium carbonate (Lowenstam and Weiner, 1989).

In crustaceans, as in all arthropods, the exoskeleton is periodically shed and rebuilt in a process known as molting, thus enabling growth. Molting is accompanied by a significant loss of cuticular calcium, quickly regained during post-molt so as to enable the animal to begin feeding. In crayfish (Travis, 1963a; Travis, 1963b), lobsters and some land crabs (Luquet and Marin, 2004), pre-molt preparation is accompanied by the formation of calcium carbonate storage organs, called gastroliths, on both sides of the stomach wall.

Like the exoskeleton, gastroliths are composed of a chitin–protein organic matrix into which calcium carbonate is deposited (Luquet

and Marin, 2004; Roer and Dillaman, 1984), and their forming epithelia are continuous. Moreover, at least two structural gastrolith proteins were identified as being expressed in the sub-cuticle epithelium as well as in the gastrolith-forming epithelium (Glazer et al., 2010; Yudkovski et al., 2010). However, gastroliths lack the structural complexity of the cuticle in terms of the four different layers typical of the cuticle, as well as other properties (Shechter et al., 2008a; Travis, 1960; Travis, 1963a). For this reason, we previously suggested that gastroliths can serve as a relatively simple extracellular model for the study of certain aspects of exoskeletal matrices in a biological system (Glazer and Sagi, 2012).

Members of the arthropod hemocyanin superfamily contribute to the cross-linking of cuticular proteins and chitins to induce cuticle hardening or sclerotization. This superfamily includes five classes of proteins, namely hemocyanins, phenoloxidases, non-respiratory crustacean cryptocyanins (pseudo-hemocyanins), insect hexamerins and hexamerin receptors (Burmester, 2002). Of these, the phenoloxidases are involved in sclerotization, in the melanin-forming pathway, in wound healing and in the humoral immune system (Burmester, 2002; Sugumaran, 1998). Moreover, phenoloxidase and hemocyanin both bind oxygen through ‘type 3’ copper-containing domains (Burmester, 2002), with hemocyanins transporting oxygen in the hemolymph of many arthropod species

(Burmester, 2002; Markl and Decker, 1992; van Holde and Miller, 1995). Crustacean phenoloxidases are derived from inactive prophenoloxidases in hemocytes (Aspán et al., 1995). These precursors are secreted into the hemolymph, where they can be activated by specific proteinases or can be deposited in the cuticle, where they are activated on site (Söderhäll and Cerenius, 1998). Crustacean hemocyanins are expressed in the hepatopancreas of several species (Adachi et al., 2005; Durstewitz and Terwilliger, 1997; van Holde and Miller, 1995) and are secreted to the hemolymph, where they occur as large extracellular multi-subunit molecules (van Holde and Miller, 1995). Hemocyanin can also be converted into phenoloxidase (Adachi et al., 2005; Adachi et al., 2001; Decker and Jaenicke, 2004). In addition, Adachi and colleagues (Adachi et al., 2005) identified hemocyanins in the cuticle of the shrimp *Penaeus japonicus*, and demonstrated the *in vitro* phenoloxidase activity of the enzyme. These authors further suggested that cuticular hemocyanin functions as a sclerotizing agent and/or an innate immunity factor.

In a study on proteins extracted from the gastrolith matrix of the crayfish *Cherax quadricarinatus*, a doublet of ~70–75 kDa was identified (Bentov et al., 2010) and later termed GAP 75 (Glazer and Sagi, 2012). At that time, the sequences of the protein and its coding transcript were not known. Accordingly, the present study focused on these protein bands and demonstrated them to contain hemocyanin proteins. The distribution of these proteins within the extracellular matrix of the gastrolith was studied immunologically. At the same time, the transcript tissue expression pattern was determined. Lastly, phenoloxidase activity of the gastrolith hemocyanin was assayed.

MATERIALS AND METHODS

Animals and molt

Cherax quadricarinatus males, supplied by Ayana Benet Perlberg of the Dor Agriculture Center (Department of Fisheries and Aquaculture, Israel Ministry of Agriculture and Rural Development), were grown in artificial ponds at Ben-Gurion University of the Negev, Beer-Sheva, Israel, under conditions described elsewhere (Shechter et al., 2008a). Inter-molt crayfish were held in individual cages and endocrinologically induced to enter pre-molt through removal of the X organ–sinus gland (XO–SG) complex or, specifically for the 454-sequencing, through daily injection of 0.3 µg α-ecdysone per 1 g animal mass. Progression of the molt cycle was monitored daily by measuring the gastrolith molt mineralization index (MMI), as described previously (Shechter et al., 2007). For all dissection procedures, crayfish were placed on ice for 5–10 min, until anesthetized.

Purification, separation and visualization of gastrolith proteins

Gastroliths were dissected from induced pre-molt crayfish, cleaned and ground to a powder in liquid nitrogen. Gastrolith proteins were extracted and separated following the procedure detailed previously (Shechter et al., 2008b). Briefly, EGTA-extracted gastrolith proteins were HPLC-separated on a DEAE column. Washes with 0.1–1 mol l⁻¹ NaCl in a step gradient with 0.1 mol l⁻¹ increments were performed. Fractions collected at 0.2–0.3 mol l⁻¹ NaCl were separated on a 9% SDS-PAGE (1.5 mm thick) gel with Tris-glycine running buffer (Laemmli, 1970). Bands were visualized by Coomassie Brilliant Blue staining (CBB).

Mass spectrometry

Reduction, alkylation and trypsinization steps were carried out as described previously (Roth et al., 2010). The resulting peptides were

loaded onto a home-made reverse-phase column (15 cm long, 75 µm internal diameter) packed with Jupiter C18, 300Å, 5 µm beads (Phenomenex, Torrance, CA, USA) and connected to a Eksigent nano-LC system (Eksigent, Dublin, CA, USA). Chromatography was performed with two solutions: buffer A (2% acetonitrile in 0.1% formic acid) and buffer B (80% acetonitrile in 0.1% formic acid), via a linear gradient (20–60%) created by buffer B over 45 min. Mass spectrometry (MS) peptide analysis and tandem MS fragmentation were performed using the LTQ-Orbitrap (Thermo Fisher Scientific, Waltham, MA, USA). The mass spectrometer was operated in the data-dependent mode to enable switching between MS and collision-induced dissociation tandem MS analyses of the top eight ions. The collision-induced dissociation fragmentation was performed at 35% collision energy with a 30 ms activation time. Proteins were identified and validated either against UniProtKB/Swiss-Prot or against an internal database containing 454-sequenced *C. quadricarinatus* hemocyanin sequences, using the Sequest algorithm operated under Proteome Discoverer 1.2 software (Thermo Fisher Scientific). The following search parameters were used: enzyme specificity trypsin, maximum two missed cleavage sites, cysteine carbamidomethylation, methionine oxidation and a maximum of 10 p.p.m. or 0.8 Da error tolerance for full scan and MS/MS analysis, respectively. Protein identification criteria were defined as having at least one peptide with a false discovery rate (FDR) *P*-value <0.01.

Western blot analysis

For western blot analyses, proteins were separated on 9% or 10% SDS-PAGE (1.5 mm thick) gels with the tricine running buffer system (Schägger and von Jagow, 1987), as described by the manufacturer, and transferred to a nitrocellulose membrane. The membrane was blocked with 5% skimmed milk in Tris-buffered saline (TBS) then incubated with anti-hemocyanin antisera (Tom et al., 1993) at a dilution of 1:1000 (v/v). After washing with TBS containing 0.1% Tween-20 (TBST), the membrane was incubated with horseradish peroxidase (HRP)-conjugated goat anti-rabbit immunoglobulin G secondary antibodies (1:15,000, v/v). Antibody binding was detected using an EZ-ECL chemiluminescence detection kit (Biological Industries, Kibbutz Beit Haemek, Israel).

Immunohistochemistry

For the immunohistochemistry assay, whole gastrolith pouches were submerged in a decalcifying fixative containing 7% EDTA and 0.2% glutaraldehyde in phosphate-buffered saline (PBS), and then dehydrated in ethanol and embedded in paraffin. Paraffin sections 5 µm thick were deparaffinized, rehydrated, incubated in citrate buffer (0.5 mol l⁻¹, pH 6.0, 30 min at 95°C) for antigen retrieval and washed in PBS (10 mmol l⁻¹, pH 7.4). Blocking (2% normal goat serum, 0.1% Triton X-100, 0.05% Tween 20 in PBS) was performed for 1 h at room temperature, followed by incubation with anti-hemocyanin antisera as primary antibodies (1:500, v/v). Slides were washed in PBS and incubated with secondary goat anti-rabbit FITC-conjugated antibodies (1:250 in PBS with 0.2% fish skin gelatin) for 1 h at room temperature. After PBS washes, slides were mounted (DAPI 1:1000 in PBS and 50% glycerol) and imaged using a fluorescence microscope.

454-Sequencing and bioinformatics analysis

RNA was extracted from the gastrolith-forming and the subcuticular epithelia pooled from crayfish at four different molt stages, namely inter-molt, early pre-molt, late pre-molt and post-molt. Five to seven animals were sampled for each molt stage. A 10 µg sample

of total RNA in H₂O was pyro-sequenced (DYN Diagnostics, Caesarea, Israel) using the GS-FLX titanium device (Roche Diagnostics, Mannheim, Germany). A 7/16 fraction of a sequencing plate was used, yielding a total of 276,377 reads, consisting of 96,748,000 bases. Sequence assembly and a Blast2GO search were performed by DYN Diagnostics. Of the 16 annotated *hemocyanin*-family sequences, the 13 unique sequences were deposited at DDBJ/EMBL/GenBank as part of a Transcriptome Shotgun Assembly (TSA) project under the accession no. GADE00000000 (the version described in this paper is the first version, GADE01000000).

Pre-molt expression pattern

To identify tissue-specific hemocyanin expression, RNA was extracted from the gastrolith-forming epithelium, sub-cuticular epithelium, hepatopancreas, muscle, testis and hemocytes. First-strand cDNA was generated with oligo (dT)₁₈VN using expand-RT reverse transcriptase (Roche Diagnostics). PCR was performed with the following primers: Hem_2_F1 (5'-CAGCGTCGTGGATCAGTTGAGGGGAAGG-3') and Hem_2_R1 (5'-CACGCCACGCTGACCACGACGATA-3') for amplification of *CqHc5*, *CqHc6* and *CqHc8* or Hem_3_F1 (5'-GCCACACCATCAACATCTTCAAAGTGTACATC-3') and Hem_3_R1 (5'-ACACTGCAAGACCTGGTCTTGCTTCGTT-3') for amplification of *CqHc2*.

Zymographic assay of phenoloxidase activity

A 30 µg sample of each protein fraction was separated on SDS-PAGE, in the presence of 0.5 mmol l⁻¹ CaCl₂, followed by transfer to a nitrocellulose membrane. The membrane was stained for phenoloxidase activity based on a previous method (Nellaiappan and Vinayagam, 1993), with modifications. Briefly, the membrane was incubated overnight at room temperature in phosphate buffer (100 mmol l⁻¹ NaHPO₄, pH 7.4) containing 0.1% SDS, 2 mmol l⁻¹ L-DOPA and 1 mmol l⁻¹ CaCl₂ until the appearance of specific purple staining.

RESULTS

SDS-PAGE separation of proteins extracted from the gastrolith matrix revealed a set of bands between 75 and 85 kDa that could be enriched and partially purified by elution from a DEAE resin with 0.2–0.3 mol l⁻¹ NaCl (Fig. 1, middle lane). These bands were excised from the gel and subjected to peptide analysis using tandem MS. Performing a Sequest search against the UniProt database revealed that the isolated bands showed moderate similarity in mass to hemocyanin proteins from three different crustaceans (Table 1). In light of this finding, hemocyanin purified from the crayfish hemolymph was also subjected to SDS-PAGE separation followed by MS analysis (Fig. 1, right lane). A similar identification pattern was obtained (Table 1).

After this initial MS identification, we considered the cross-reactivity of the crayfish proteins by western blot analysis using anti-hemocyanin antiserum raised against hemolymph hemocyanin of the shrimp *Penaeus semisulcatus* (Tom et al., 1993) (Fig. 2A). The antibodies cross-reacted with both hemolymph and gastrolith hemocyanins from our crayfish but not with BSA, a negative control. We then employed the antibodies in an immunohistochemical assay performed on sections of decalcified gastrolith pouches. Hematoxylin and eosin (H&E) staining (Fig. 2B, left panel) shows the chitin layers forming the gastrolith matrix surrounded by the gastrolith-forming epithelium and its attached connective tissue. Green fluorescence indicates that the protein is present throughout the width of the chitinous structure but is especially concentrated

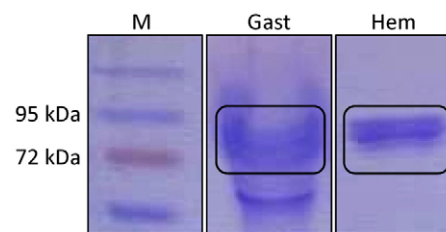


Fig. 1. SDS-PAGE separation followed by Coomassie Brilliant Blue (CBB) staining of gastrolith 75–85 kDa bands (Gast, middle) and hemolymph hemocyanin (Hem, right). The bands in each lane were excised as marked by the rectangles, trypsinized and sequenced by mass spectrometry (see also Table 1). M, molecular mass markers.

along specific chitin layers (Fig. 2B, middle image). Weak immunostaining was also observed in the cytoplasm but not in the nuclei of the gastrolith-forming epithelium cells, while a stronger reaction was seen in the surrounding connective tissue (Fig. 2B, middle and right panels).

Next-generation 454-sequencing was performed on RNA extracts of gastrolith-forming and sub-cuticular epithelia pooled from crayfish in four different molt stages, namely inter-molt, early pre-molt, late pre-molt and post-molt. Following assembly and translation, Blast2GO analysis was performed on 3520 isotig sequences against the UniProt database (Fig. 3A). Of the total number of isotigs obtained, 43% did not show similarity to any other protein in the database, 3% were similar to predicted/hypothetical proteins and 54% showed significant similarity to annotated sequences (Fig. 3A, left). The annotated sequences were grouped according to their predicted biological function, including a group of 16 sequences that were annotated as proteins from the hemocyanin family, with different sequencing coverage (Fig. 3A, right). Of the 16 hemocyanin-family isotigs, 12 were identified as hemocyanin, three as *C. quadricarinatus* cryptocyanin (CqCc) and one as *C. quadricarinatus* prophenoloxidase (CqPPO) (Fig. 3B). Four of the 12 hemocyanin isotigs were found to be identical and were,

Table 1. Liquid chromatography–tandem mass spectrometry analysis of the gastrolith 75–85 kDa bands and hemolymph hemocyanin

Protein	Peptide sequence	Peptide mass (Da)	XCorr
Gastrolith			
Asl b	DSYGYHLDR	1125.5	2.66
	DPSFFR	768.37	1.47
Cdes c	QHDVNYLLFK	1276.68	2.39
CaeSS2	YMDNIFR	974.45	2.27
	DPAFFR	752.38	1.66
	DSLTPYTK	924.47	1.05
Hemolymph			
Cdes c	QHDVNYLLFK	1276.68	2.77
Cdes a	QHDINLLFK	1274.7	2.5
Pint b	HWFSLFNTR	1207.6	2.36
	FNLPPGVMEHFETATR	1861.9	2.14
Pint c	YMDNIFR	974.45	2.05
	DPSFFR	768.37	1.96

Proteins identified: *Astacus leptodactylus* hemocyanin B chain (Asl b), *Cherax destructor* hemocyanin C chain (Cdes c), *Carcinus aestuarii* structural subunit 2 (CaeSS2), *C. destructor* hemocyanin A chain (Cdes a), *Panulirus interruptus* hemocyanin B chain (Pint b) and *P. interruptus* hemocyanin C chain (Pint c). Hemolymph hemocyanin served as a positive control.

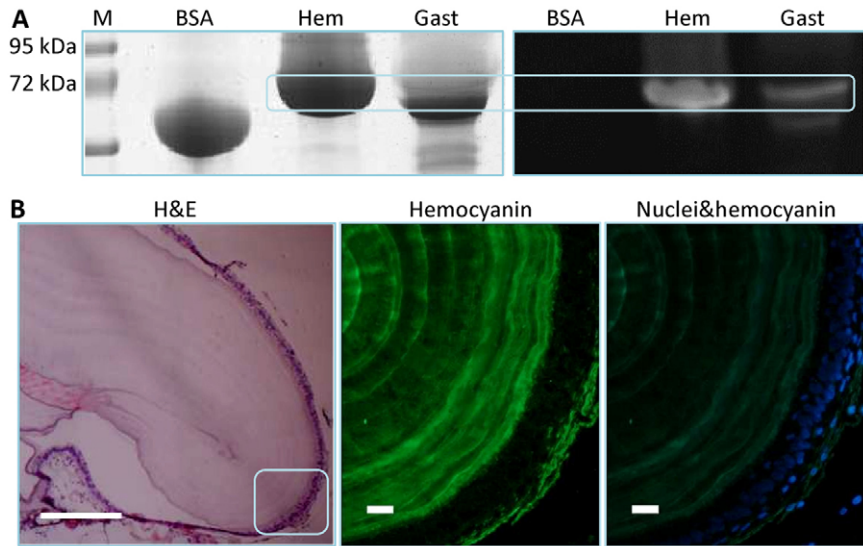


Fig. 2. Gastrolith hemocyanins identified by western blot analysis (A) and immunohistochemistry (B). (A) Left panel, CBB-stained SDS-PAGE gel of BSA, hemolymph (Hem) and gastrolith proteins (Gast). Right panel, western blot with anti-hemocyanin antibodies. (B) Left panel, hematoxylin and eosin (H&E) staining of the gastrolith pouch (bar, 200 μ m; boxed area is magnified in middle and right panels). Middle panel, hemocyanins observed in the gastrolith matrix, as well as the cytoplasm of gastrolith-forming epithelium and adjacent connective tissue cells, as demonstrated by the binding of goat anti-rabbit FITC-conjugated antibodies (bar, 25 μ m). Right panel, a merged image of hemocyanins identified by FITC and of DAPI counterstain used to identify nuclei in the gastrolith-forming epithelium and connective tissue (bar, 25 μ m).

therefore, designated as a single sequence, resulting in a total of nine unique *C. quadricarinatus* hemocyanins (CqHc). Table 2 presents a new Sequest search, based on the same MS data obtained from the bands shown in Fig. 1; this time, however, we used the assembled and annotated 454-sequencing isotigs as the database. Of the nine CqHc predicted proteins, seven were identified in the

gastrolith-extracted protein profile. The same hemocyanin proteins were also identified in the hemolymph hemocyanin extraction, along with an additional eighth protein, unique to this fraction.

The expression pattern of *hemocyanin* mRNAs was tested in pre-molt crayfish by RT-PCR in several different tissues. This revealed that *hemocyanin* transcripts were specifically expressed in the

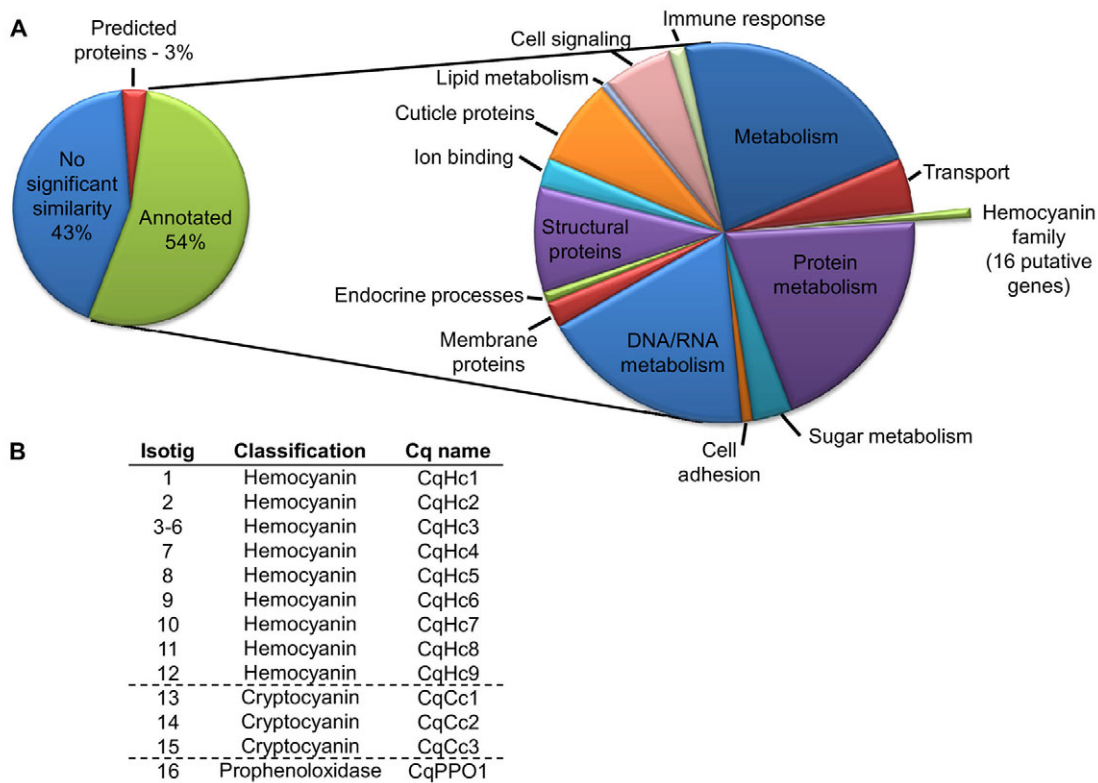


Fig. 3. *Hemocyanin*-family transcripts identified by 454-sequencing. (A) Blast2GO analysis of 3520 putative genes (isotigs) from 454-sequencing of *C. quadricarinatus* gastrolith-forming and sub-cuticular epithelia. Left, 43% of the sequences showed no significant similarity to any protein in the UniProt database, 3% were similar to predicted proteins and 54% were similar to annotated proteins. Right, GO (gene ontology) categories of the annotated sequences, including 16 putative *hemocyanin*-family transcripts. (B) List of the 16 isotigs identified as putative *hemocyanin*-family transcripts, their specific annotation and Cq (*C. quadricarinatus*) name. The 13 final sequences in the table were deposited at DDBJ/EMBL/GenBank under the accession number GADE01000000.

Table 2. Specific mass spectrometry-based identification of *C. quadricarinatus* hemocyanin-derived peptides in gastrolith 75–85 kDa bands and hemolymph hemocyanin using 454-sequencing results as the database

Protein	Molecular mass (kDa)	No. amino acids	Sequest score	No. peptides	No. unique peptides
Gastrolith					
CqHc4	76.8	673	164.11	20	9
CqHc2	76.8	669	155.67	28	18
CqHc5	76.1	659	73.31	13	9
CqHc1	77.5	674	62.31	28	26
CqHc6	75.4	659	60.31	9	1
CqHc7	75.7	659	58.47	8	1
CqHc3	59.2	510	29.56	17	13
Hemolymph					
CqHc1	77.5	674	545.81	34	34
CqHc2	76.8	669	310.94	27	16
CqHc3	59.2	510	304.05	23	23
CqHc4	76.8	673	269.54	24	13
CqHc5	76.1	659	191.35	33	25
CqHc6	75.4	659	174.51	22	4
CqHc7	75.7	659	165.34	23	6
CqHc8	29.3	255	27.41	4	4

Cherax quadricarinatus hemocyanin (CqHc) proteins were numbered according to Sequest scores calculated for the hemolymph proteins. 'No. peptides' includes only those peptides with XCorr>1. 'No. unique peptides' refers to those peptides not shared with other protein hits.

hepatopancreas (Fig. 4, upper panel). No expression was detected in any other tissues, including both epithelial tissues (i.e. the gastrolith-forming and sub-cuticular epithelia) and hemocytes.

Finally, gastrolith hemocyanin, as visualized by CBB staining following SDS-PAGE (Fig. 5A), was tested for phenoloxidase activity in the presence of SDS, L-DOPA and Ca²⁺ (Fig. 5B). Strong activity was detected in the enriched and purified fraction of gastrolith hemocyanin, as reflected by the appearance of two distinct bands (Fig. 5A,B, lane 1). The specificity of the reaction within the EGTA-soluble gastrolith protein population is demonstrated in lane 2, where the band at position 'a', containing gastrolith hemocyanins, displays strong phenoloxidase activity, while the band at position 'b', containing another protein named GAP 65, is not active. In these experiments, hemolymph hemocyanin served as a positive control (Fig. 5A,B, lane 3), while BSA served as a negative control (Fig. 5A,B, lane 4). Western blot analysis confirmed the identity of the hemocyanin bands (Fig. 5C).

DISCUSSION

In this study, we revealed the presence of hemocyanin proteins in the extracellular matrix of gastroliths deposited by the crayfish *C. quadricarinatus*. This identification results from the extensive mapping of the *C. quadricarinatus* gastrolith proteome and transcriptome we are currently performing, using the gastrolith as a simple model to study the involvement of proteins in crustacean skeletal construction. Initial identification of the proteins considered in this study was achieved by MS, as part of the proteomic mapping process, and was further supported by western blot analysis. The transcriptomic mapping yielded the partial sequences of nine hemocyanin transcripts, with the protein products of seven of them being found in the gastrolith matrix.

Our RT-PCR assay revealed that hemocyanin transcripts were uniquely expressed in the hepatopancreas during pre-molt. Specific expression in the hepatopancreas was also demonstrated for the freshwater crayfish *Pacifastacus leniusculus* by northern blot analysis (Lee et al., 2004) and for *Astacus leptodactylus* by immunoprecipitation (Gellissen et al., 1991). No expression was detected in the hemocytes of any crayfish, although in the prawn *P. japonicus*, hemocyanin expression was detected by RT-PCR in hemocytes, as well as in the hepatopancreas (Adachi et al., 2005). Furthermore, the protein was extracted from the cuticle of the prawn and immunolocalized to the exocuticular and endocuticular layers, leading the authors to suggest that cuticular hemocyanin is mainly synthesized in the hepatopancreas, from where it is transferred through the hemolymph and via the epidermal layer underlying the cuticle to the exoskeleton (Adachi et al., 2005). We offer a similar scenario for gastrolith hemocyanins, providing some support with the presence of the protein in the connective tissue surrounding the gastrolith pouch, as well as in the cytoplasm of the gastrolith-forming cells, as revealed by immunolocalization. Specific expression in the hepatopancreas, however, does not fully coincide with the tissues from which we obtained our hemocyanin transcripts, namely the gastrolith-forming and sub-cuticular epithelia. As the gastrolith-forming epithelium is highly penetrated by hemocytes ('blood cells') (Ueno, 1980), hemocyanin expression was sought but not detected in these cells. The most probable explanation for this apparent contradiction is the sequencing of residual transcript expression. Sequencing of transcripts that are expressed in very small copy numbers, and are actually non-functional, may be the result of the new next-generation sequencing methods, such as 454-sequencing, given their vast sequencing depth. Transcript

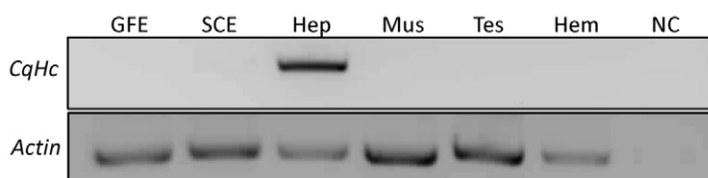


Fig. 4. *CqHc* expression patterns in various crayfish tissues, as demonstrated by RT-PCR (upper panel). Total RNA was extracted from pre-molt gastrolith-forming epithelium (GFE), sub-cuticular epithelium (SCE), hepatopancreas (Hep), muscle (Mus), testes (Tes) and hemocytes (Hem). Actin was used to confirm RNA extraction (lower panel). RNA from the hepatopancreas served as a negative control (NC), to rule out genomic contamination.

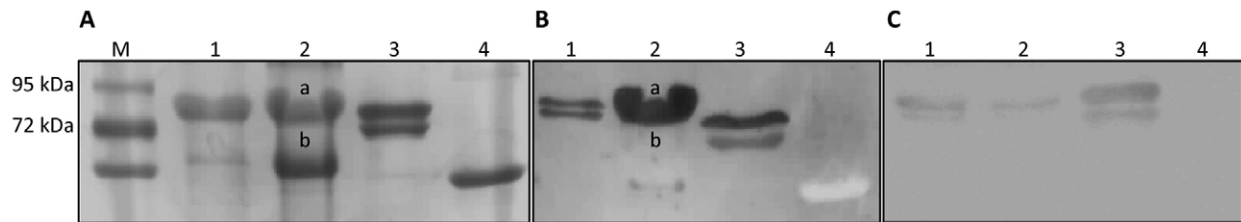


Fig. 5. Phenoloxidase activity of gastrolith hemocyanin. SDS-PAGE-separated, DEAE-purified gastrolith hemocyanin (1), total gastrolith soluble proteins (2), hemolymph hemocyanin (3) and BSA (4), stained with CBB (A), transferred to nitrocellulose membranes and subjected to phenoloxidase enzyme assay (B) or probed with anti-hemocyanin antibodies (C). Bands marked by a and b are hemocyanins and GAP 65 (respectively), as they appear in the total gastrolith soluble protein profile.

expression experiments using the RNA-seq analytical procedure may prove the presented assumption by quantifying the expression.

The presence of hemocyanins in the chitinous matrix of a temporary calcium storage organ, such as the gastrolith, raises the question of the role of hemocyanins in this structure. One possible explanation is that these hemolymph-circulating proteins diffuse into the growing matrix through the open vascular system penetrating the forming epithelium, possibly acting as transporters of oxygen or even of ecdysone (Jaenicke et al., 1999). The hemocyanins would thus be trapped within the chitin network as the layers rapidly accumulate. A second explanation is that hemocyanins play a structural role, perhaps as sclerotizing agents hardening the 3D chitinous network that serves as a solid scaffold for deposition of stored calcium. In her work on the Dungeness crab, *Cancer magister*, Terwilliger (Terwilliger, 2007) suggested that crab hemocyanin may be converted from transporting oxygen to functioning as a phenoloxidase during molting, when there is a need for concerted and rapid sclerotization. In an earlier work, Terwilliger and colleagues (Terwilliger et al., 2005) showed in juvenile crabs that the hemolymph concentration of hemocyanin cyclically decreased at ecdysis, and increased as pre-molt progressed until the next molt event. At the transcript level, *hemocyanins* of the crab *Portunus pelagicus* showed high levels of expression in the inter-molt and pre-molt stages, when compared with ecdysis and post-molt (Kuballa and Elizur, 2008; Kuballa et al., 2011). In *C. quadricarinatus*, a microarray experiment comparing hepatopancreas gene expression in inter-molt *versus* pre-molt and post-molt animals indicated a reduction in the transcription levels of one *hemocyanin* gene in inter-molt, while another *hemocyanin* gene was most highly transcribed in inter-molt (Yudkovski et al., 2007). In the present study, hemocyanin was observed within the gastrolith matrix, showing a distribution pattern with seemingly higher concentrations of the protein along certain chitin-formed layers. The observed pattern could be due to changes in composition along the gastrolith vertical axis or perhaps fluctuations in the rate of layer formation and secretion of matrix ingredients from the forming epithelium. In addition, some protein may have been extracted during decalcification despite the use of fixative along with the decalcifying solution. Gastrolith formation and molting can be naturally achieved in juvenile crustaceans within a few days to 2 weeks (as per our observations), a process that in adult crustaceans may take as long as 2 months (Skinner, 1985). To date, there are no published data elaborating on the manner and/or rate in which gastrolith chitin layers are formed. In any case, it is a continuous process that requires fast maturation of each newly formed stratum while the next is already being secreted and, therefore, is likely to involve a set of hardening factors working in concert, including

converted hemocyanins. Indeed, we found that our gastrolith hemocyanins can function as phenoloxidases in the presence of SDS, as was shown previously (Adachi et al., 2005) for cuticular hemocyanins.

In conclusion, it is already widely agreed that crustacean hemocyanins are not restricted to serving oxygen-carrying roles alone but can play a much wider array of roles that vary according to the animal's physiological status. Moreover, the location of crustacean hemocyanins is not restricted to the hemolymph, as they may be transferred to other tissues, where they can perform other functions. Accordingly, we detected several hemocyanins in the gastrolith matrix, a non-cellular temporary structure, where they may be maintained for the purpose of forming a rigid construct for calcium storage. As such, we propose that the presence of hemocyanins in the gastrolith may be required for fast hardening of the chitin scaffold in the highly dynamic process of gastrolith formation; however, other possible functions cannot be excluded.

ACKNOWLEDGEMENTS

We thank Aviv Ziv, Tom Levi and Omri Lapidot for technical assistance. We thank Ayana Benet Perlberg of the Dor Agriculture Center, Department of Fisheries and Aquaculture, Israel Ministry of Agriculture and Rural Development, for the supplied animals.

AUTHOR CONTRIBUTIONS

The experimental work, analysis and writing of the results were performed by L.G. and led by A.S. The 454-sequencing process was coordinated and led by M.T. Protein biochemistry was performed largely by S.W., with the participation of B.M. Mass spectrometry analysis was performed in collaboration with Z.R. and I.K.

COMPETING INTERESTS

No competing interests declared.

FUNDING

This work was supported by the Israel Science Foundation [grant no. 102/09].

REFERENCES

- Adachi, K., Hirata, T., Nagai, K. and Sakaguchi, M. (2001). Hemocyanin a most likely inducer of black spots in kuruma prawn *Penaeus japonicus* during storage. *J. Food Sci.* **66**, 1130-1136.
- Adachi, K., Endo, H., Watanabe, T., Nishioka, T. and Hirata, T. (2005). Hemocyanin in the exoskeleton of crustaceans: enzymatic properties and immunolocalization. *Pigment Cell Res.* **18**, 136-143.
- Aspán, A., Huang, T. S., Cerenius, L. and Söderhäll, K. (1995). cDNA cloning of prophenoloxidase from the freshwater crayfish *Pacifastacus leniusculus* and its activation. *Proc. Natl. Acad. Sci. USA* **92**, 939-943.
- Bentov, S., Weil, S., Glazer, L., Sagi, A. and Berman, A. (2010). Stabilization of amorphous calcium carbonate by phosphate rich organic matrix proteins and by single phosphoamino acids. *J. Struct. Biol.* **171**, 207-215.
- Blackwell, J. and Weih, M. A. (1980). Structure of chitin-protein complexes: ovipositor of the ichneumon fly *Megarhyssa*. *J. Mol. Biol.* **137**, 49-60.
- Bouligand, Y. (1972). Twisted fibrous arrangements in biological materials and cholesteric mesophases. *Tissue Cell* **4**, 189-217.
- Burmester, T. (2002). Origin and evolution of arthropod hemocyanins and related proteins. *J. Comp. Physiol. B* **172**, 95-107.

- Decker, H. and Jaenicke, E. (2004). Recent findings on phenoloxidase activity and antimicrobial activity of hemocyanins. *Dev. Comp. Immunol.* **28**, 673-687.
- Durstewitz, G. and Terwilliger, N. B. (1997). Developmental changes in hemocyanin expression in the Dungeness crab, *Cancer magister*. *J. Biol. Chem.* **272**, 4347-4350.
- Gellissen, G., Hennecke, R. and Spindler, K. D. (1991). The site of synthesis of hemocyanin in the crayfish, *Astacus leptodactylus*. *Experientia* **47**, 194-195.
- Glazer, L. and Sagi, A. (2012). On the involvement of proteins in the assembly of the crayfish gastrolith extracellular matrix. *Invertebr. Reprod. Dev.* **56**, 57-65.
- Glazer, L., Shechter, A., Tom, M., Yudkovski, Y., Weil, S., Afialo, E. D., Pamuru, R. R., Khalaila, I., Bentov, S., Berman, A. et al. (2010). A protein involved in the assembly of an extracellular calcium storage matrix. *J. Biol. Chem.* **285**, 12831-12839.
- Jaenicke, E., Föll, R. and Decker, H. (1999). Spider hemocyanin binds ecdysone and 20-OH-ecdysone. *J. Biol. Chem.* **274**, 34267-34271.
- Kuballa, A. V. and Elizur, A. (2008). Differential expression profiling of components associated with exoskeletal hardening in crustaceans. *BMC Genomics* **9**, 575.
- Kuballa, A. V., Holton, T. A., Paterson, B. and Elizur, A. (2011). Moulting cycle specific differential gene expression profiling of the crab *Portunus pelagicus*. *BMC Genomics* **12**, 147.
- Laemmli, U. K. (1970). Cleavage of structural proteins during the assembly of the head of bacteriophage T4. *Nature* **227**, 680-685.
- Lee, S. Y., Lee, B. L. and Söderhäll, K. (2004). Processing of crayfish hemocyanin subunits into phenoloxidase. *Biochem. Biophys. Res. Commun.* **322**, 490-496.
- Lowenstam, H. A. and Weiner, S. (1989). *On Biomineralization*. New York, NY: Oxford University Press.
- Luquet, G. and Marin, F. (2004). Biomineralisations in crustaceans: storage strategies. *C. R. Palevol.* **3**, 515-534.
- Markl, J. and Decker, H. (1992). Molecular structure of the arthropod hemocyanins. *Adv. Comp. Environ. Physiol.* **13**, 325-376.
- Nellaippan, K. and Vinayakam, A. (1993). A method for demonstrating phenoloxidase after electrophoresis. *Biotech. Histochem.* **68**, 193-195.
- Raabe, D., Romano, P., Sachs, C., Al-Sawalmih, A., Brokmeier, H. G., Yi, S. B., Servos, G. and Hartwig, H. G. (2005). Discovery of a honeycomb structure in the twisted plywood patterns of fibrous biological nanocomposite tissue. *J. Cryst. Growth* **283**, 1-7.
- Roer, R. and Dillman, R. (1984). The structure and calcification of the crustacean cuticle. *Am. Zool.* **24**, 893-909.
- Roth, Z., Parnes, S., Wiel, S., Sagi, A., Zmora, N., Chung, J. S. and Khalaila, I. (2010). N-glycan moieties of the crustacean egg yolk protein and their glycosylation sites. *Glycoconj. J.* **27**, 159-169.
- Schägger, H. and von Jagow, G. (1987). Tricine-sodium dodecyl sulfate-polyacrylamide gel electrophoresis for the separation of proteins in the range from 1 to 100 kDa. *Anal. Biochem.* **166**, 368-379.
- Shechter, A., Tom, M., Yudkovski, Y., Weil, S., Chang, S. A., Chang, E. S., Chalifa-Caspi, V., Berman, A. and Sagi, A. (2007). Search for hepatopancreatic ecdysteroid-responsive genes during the crayfish molt cycle: from a single gene to multigenicity. *J. Exp. Biol.* **210**, 3525-3537.
- Shechter, A., Berman, A., Singer, A., Freiman, A., Grinstein, M., Erez, J., Afialo, E. D. and Sagi, A. (2008a). Reciprocal changes in calcification of the gastrolith and cuticle during the molt cycle of the red claw crayfish *Cherax quadricarinatus*. *Biol. Bull.* **214**, 122-134.
- Shechter, A., Glazer, L., Chaled, S., Mor, E., Weil, S., Berman, A., Bentov, S., Afialo, D. E., Khalaila, I. and Sagi, A. (2008b). A gastrolith protein serving a dual role in the formation of extracellular matrix containing an amorphous mineral. *Proc. Natl. Acad. Sci. USA* **105**, 7129-7134.
- Skinner, D. M. (1985). Molting and regeneration. In *The Biology of Crustacea*, Vol. 9 (ed. D. E. Bliss), pp. 44-128. New York, NY: Academic Press.
- Söderhäll, K. and Cerenius, L. (1998). Role of the prophenoloxidase-activating system in invertebrate immunity. *Curr. Opin. Immunol.* **10**, 23-28.
- Sugumaran, M. (1998). Unified mechanism for sclerotization of insect cuticle. *Adv. Insect Physiol.* **27**, 229-334.
- Terwilliger, N. B. (2007). Hemocyanins and the immune response: defense against the dark arts. *Integr. Comp. Biol.* **47**, 662-665.
- Terwilliger, N. B., Ryan, M. C. and Towle, D. (2005). Evolution of novel functions: cryptocyanin helps build new exoskeleton in *Cancer magister*. *J. Exp. Biol.* **208**, 2467-2474.
- Tom, M., Shenker, O. and Ovadia, M. (1993). Partial characterization of 3 hemolymph-proteins of *Penaeus semisulcatus* Dehaan (Crustacea, Decapoda, Penaeidae) and their specific antibodies. *Comp. Biochem. Physiol.* **104B**, 811-816.
- Travis, D. F. (1960). The deposition of skeletal structures in the Crustacea. 1. The histology of the gastrolith skeletal tissue complex and the gastrolith in the crayfish, *Orconectes (cambaus) virilis* Hagen – Decapoda. *Biol. Bull.* **118**, 137-149.
- Travis, D. F. (1963a). The deposition of skeletal structures in the crustacea. 2. The histochemical changes associated with the development of the nonmineralized skeletal components of the gastrolith discs of the crayfish, *Orconectes virilis hagen*. *Acta Histochem.* **15**, 251-268.
- Travis, D. F. (1963b). The deposition of skeletal structures in the Crustacea. 3. The histochemical changes associated with the development of the mineralized gastroliths in the crayfish, *Orconectes virilis hagen*. *Acta Histochem.* **15**, 269-284.
- Ueno, M. (1980). Calcium-transport in crayfish gastrolith disk – morphology of gastrolith disk and ultrahistochemical demonstration of calcium. *J. Exp. Zool.* **213**, 161-171.
- van Holde, K. E. and Miller, K. I. (1995). Hemocyanins. *Adv. Protein Chem.* **47**, 1-81.
- Yudkovski, Y., Shechter, A., Chalifa-Caspi, V., Auslander, M., Ophir, R., Dauphin-Villemant, C., Waterman, M., Sagi, A. and Tom, M. (2007). Hepatopancreatic multi-transcript expression patterns in the crayfish *Cherax quadricarinatus* during the molt cycle. *Insect Mol. Biol.* **16**, 661-674.
- Yudkovski, Y., Glazer, L., Shechter, A., Reinhardt, R., Chalifa-Caspi, V., Sagi, A. and Tom, M. (2010). Multi-transcript expression patterns in the gastrolith disk and the hypodermis of the crayfish *Cherax quadricarinatus* at premolt. *Comp. Biochem. Physiol.* **5D**, 171-177.